Journal of Engineering and Technology Research Vol. 3(6), pp. 180-196, June 2011
Available online at http:// www.academicjournals.org/JETR
ISSN 2006-9790 ©2011 Academic Journals

Full Length Research Paper

Opto-mechanical design, analysis and economical manufacture of a large aperture LIDAR receiver telescope

T. Bangia[1,2]*, P. K. Agarwal[3], A. Kumar[1], S. K. Singh[1] and R. Sagar[1]

[1]Aryabhatta Research Institute of observational sciencES (ARIES), Manora Peak, Nainital, Uttarakhand 263 129, India.
[2]Uttar Pradesh Technical University, (UPTU), Lucknow, Uttar Pradesh 226021, India.
[3]Ideal Institute of Management and Technology, Ghaziabad, Uttar Pradesh 201003, India.

Accepted 28 April, 2011

Aryabhatta Research Institute of Observational Sciences (ARIES) at Nainital (29° 22' N, 79° 27' E, 1950 m amsl) is located in the central Himalayan region. Taking benefit of its pristine geographical location away from major urban pollution a LIDAR system was planned at this location to study the dynamics of atmosphere. Optical design analysis of LIDAR receiver telescope with backend detection optics was carried out in ZEMAX - EE simulation package to optimize system parameters. A concave mirror of 840 mm diameter was used as primary mirror to develop a large aperture LIDAR receiver telescope for receiving back-scattered photons from atmosphere. Mirror was housed in a simple three piece mirror cell manufactured precisely and economically from cast aluminium alloy 535.0 by Lost - Foam casting process. Mirror was kept floating at 18 points on axial supports designed, analyzed and manufactured for maintaining the optical quality of telescope. Solid modeling and deflection analysis of the axial supports confirmed that deflection due to mirror weight was within 10 µ whose effect on degradation of optical parameters was analyzed and found quite negligible.

Key words: Telescope, LIDAR, lost - foam casting (LFC), axial supports.

INTRODUCTION

Light detection and ranging (LIDAR) probing is one of the most successful active remote sensing techniques for atmospheric studies. Two groups at Hughes Aircraft Malibu and Culver City pioneered the construction of LIDAR system in 1961 for range finding applications. LIDAR studies were subsequently carried out by using a ruby light amplification by stimulated emission of radiation (LASER) as a source (Ligda, 1963; Fiocco and Smullin, 1963; Fiocco and Grams, 1964). Recent studies have taken advantage of high power pulsed Neodymium (Nd) - yttrium aluminum garnet (YAG) LASER (Chanin et al., 1981). Atmospheric LIDAR is generally used to probe vertical distribution of aerosols and molecules by sending a pulsed LASER beam vertically up in the atmosphere. Back-scattered photons from atmosphere are collected using a receiver telescope (Weitkamp, 2005). Photons are detected and measured using a detection system. Backscattered signal strength is proportional to amount of scatterers at a particular altitude. Time delay between the transmitted pulse and arrival time of backscattered signal gives the altitude information.

India is among one of the fastest growing economies in world and its climate is significantly getting affected by rapid industrialization and urbanization. Location of Indian subcontinent extending from Kanyakumari, almost at the magnetic equator (8° 4' N) to Kashmir in the north (34° 03' N) provides a unique opportunity to study atmospheric sciences in India. Atmospheric studies at India include meteorology (Jayaraman et al., 2007), ionosphere investigations (Dabas et al., 2008), geomagnetism (Waghmare et al., 2008) and solar-terrestrial relations (Pillai et al., 2003). ARIES located in the central Himalayan region is a mid-latitude and high altitude site in the country. ARIES has made unique contribution in many areas of astronomical research due to its imperative geographical location, particularly those involving time critical phenomena (Sagar, 2006). The site is reasonably away from major urban pollution making it

*Corresponding author. E-mail: bangia@aries.res.in

suitable to monitor and study aerosol (particles of solid or liquid phase dispersed in the atmosphere) loading of the atmosphere (Sagar, 2004) and to understand regional influence on climate variability. Considering the geographical location of ARIES a ground based LIDAR system was recently installed at this site. LIDAR system designed at ARIES consists of three subsystems namely transmitter, receiver and detection system (Liu et al., 2007). Transmitter is a Q-switched Nd: YAG LASER, emitting linearly polarized pulses. Receiver consists of a Newtonian telescope and detection system comprising of photo multiplier Tube (PMT), discriminator and a PCI based multi-channel scaler (MCS).

Receiver in ground based LIDAR system generally consists of Cassegrain or Newtonian telescope (Velotta et al., 1998). Newtonian telescopes are usually less expensive for any given aperture than comparable quality telescopes of other types (Schwab, 2003). Also short focal ratio allows compact mounting system, reducing cost and increasing portability. The present paper highlights the optimized indigenous design, analysis and economical manufacture of LIDAR receiver telescope using a concave mirror of 840 mm diameter with 1428 mm (f/1.7) focal length. Instead of conventional heavy weight single piece primary mirror cell (Bely, 2003) a light weight three piece cell was designed and manufactured quite precisely and economically using evaporative LFC process. A gimbal mounted elliptical plane mirror of 475 X 375 mm with five axis motion was used as secondary mirror for the telescope. Axial supports were designed, analyzed and manufactured for large diameter mirror to achieve floating condition for the mirror (Bely, 2003). Deflection in mirror supports can result in appreciable degradation in image quality (Nelson et. al., 1982). Effect of deflection in axial supports was analyzed to calculate encircled energy, spot diagrams, variation of RMS wavefront error and distortion in image.

MATERIALS AND METHODS

Optical design and analysis

The optical design optimization and analysis for receiver telescope and back end optics of LIDAR was carried out by using ZEMAX-EE simulation package. The optical layout, encircled energy, spot diagrams, variation of RMS wavefront error and distortion were simulated by taking the optical parameters of system (Boyarchuk et al., 2008). The result depicts that rays after reflection from primary mirror are intercepted by the secondary mirror before the prime focus. Secondary mirror sends the rays outside the side of tube which are then focused on to the focal plane of PMT through detection optics comprising of collimating lenses and a narrow band interference filter at 532 nm (Figure 1).

Encircled energy, f is defined as:

$$f = \frac{\int_0^r I(r)dr}{\int_0^\infty I(r)dr} \quad (1)$$

where, I(r) is the fraction of total energy, contained within a circle of a specified radius r, centered on the chief ray reference point and it varies between 0 and 1. The radial coordinate at which a specified fraction can be achieved was computed by variation of encircled energy with fields. It was concluded from the plot that 80% of encircled energy at 0.00°field lies in 52.36 µ radius (Figure 2).

Spot diagrams for three fields at 0.00, 0.35 and 0.50° were analyzed. Root mean square (RMS) radius depends upon every ray and gives an idea of spread of the rays. GEO radius is radius of circle centered at the reference point enclosing all the rays. RMS spot size varied from 7390.49 to 6899.84 µ and GEO radius varied from 7689.82 to 7679.39 µ for the variation in field from 0.00 to 0.50°(Figure 3).

Variation of RMS wavefront error in waves with field was determined and found to vary marginally from 0.081 to 0.070 waves with variation in field from 0.00 to 0.50°(Figure 4a). Strehl ratio that evaluates the optical quality of telescope is determined from RMS wavefront error. Strehl ratio changed from 0.768 to 0.827 with variation in field from 0.00 to 0.50° (Figure 4b). Distortion that measures the deviation between the reference and actual image height was determined as 1.31% (Figure 4c).

Mechanical design and manufacture

LIDAR receiver telescope is the prime requirement for most of the ground based LIDAR systems. By convention any mirror larger than 380 mm diameter should be provided with mechanical flotation and adequate edge support. The mirror must rest on a number of self - adjusting supports, geometrically symmetrical with each other and each taking an equal share of the weight (Hindle, 1996). The concave mirror of 840 mm diameter and 140 mm thickness made it imperative to have perfect mirror supports for converting it in to a Newtonian telescope. It belongs to the category of monolithic mirrors (diameter to thickness ratio of 6:1) that are made thick and stiff to avoid flexures. Newtonian telescope was designed and manufactured with following main components:

Primary mirror cell

Primary mirror cell is the most important and sensitive part of a telescope (Meinel, 1977). Primary mirror cells in one meter class telescopes are conventionally designed in a single piece and are generally one of the heaviest parts in a telescope mechanical structure (Bely, 2003). The weight of the primary mirror cell is coupled to the primary mirror for supporting it with precision during motion. However, design considerations behind primary mirror cell for stationary LIDAR receiver telescope were light in weight, simplified design, low cost of manufacture, easy to assemble /disassemble and durable to withstand the primary mirror weight of 180 kg. Primary mirror cell is required to precisely position the mirror on supports. Primary mirror cell was designed in three components and has provision for accommodating axial and radial supports for primary mirror. It consists of a cylindrical shell mounted on a base plate with a circular ring at the top. Cylindrical shell of outer diameter 1000 mm and height 255 mm was designed with provision for six radial supports to support the primary mirror at its circumference. A base plate of diameter 1000 mm and thickness 35 mm was fastened to bottom of the shell. It has provision for incorporating 18 axial supports to hold primary mirror from back. Base plate is designed with feet having adjustable vibration dampeners for leveling and dampening of vibrations. A 35 mm thick circular ring of outer diameter 990 mm was fastened on shell top to protect mirror from coming out if mirror cell is tilted.

Three components of primary mirror cell were manufactured from cast aluminium alloy 535.0 by LFC process, which is a type of

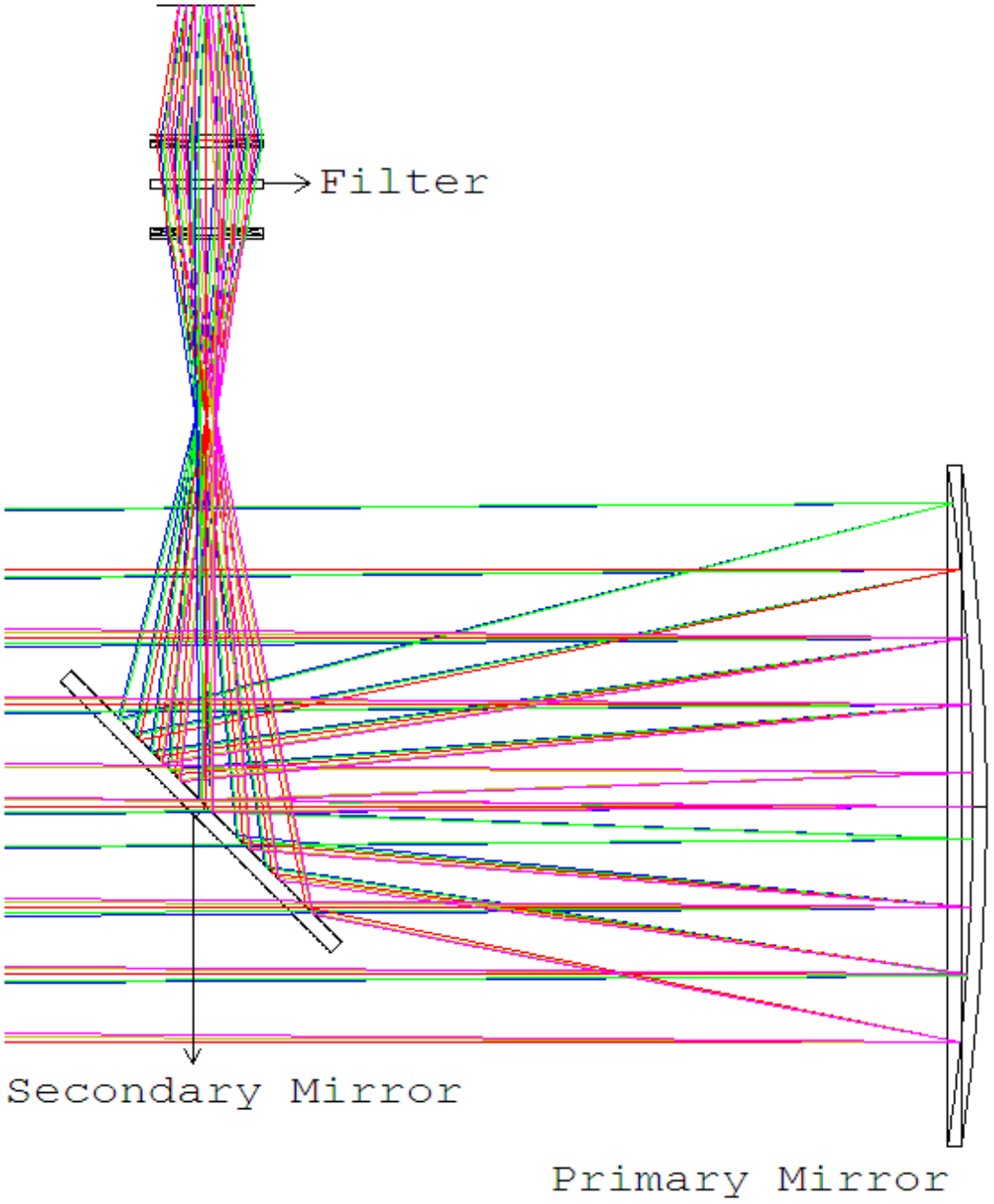

Figure 1. Optical layout of the system.

evaporative pattern casting process utilizing foam as the pattern material. The process proved to be quite simple, precise, fast and inexpensive for producing mirror cell with excellent surface finish. Aluminium alloy 535.0 contains 92.84% Al, 6.80% Mg, 0.18% Mn and 0.18% Ti. Its tensile strength is 275 MPa and yield strength is 140 MPa (Chandler, 2006). This aluminium - magnesium alloy possesses a combination of strength and ductility. It is appropriate for parts in instruments where dimensional stability is of major importance. It has high corrosion resistance and excellent machinability. LFC process employed expanded polystyrene foam patterns that vaporized during pouring of molten metal (Niemann, 1998). Patterns for three components of primary mirror cell were prepared quite economically using a hot - wire foam cutter keeping in view the machining allowances. Casted components were further finish machined to desired dimensions for achieving final sizes of the components.

Axial supports for the primary mirror

Primary mirror is supported on two types of supports, that is, axial and radial supports. Supports must hold the mirror within few microns of its aligned position without exerting any pressure on it. Pressure deforms the mirror and results in noticeable optical aberrations. Axial supports take weight acting along axis of the mirror. Total force provided by axial supports varies as a function of

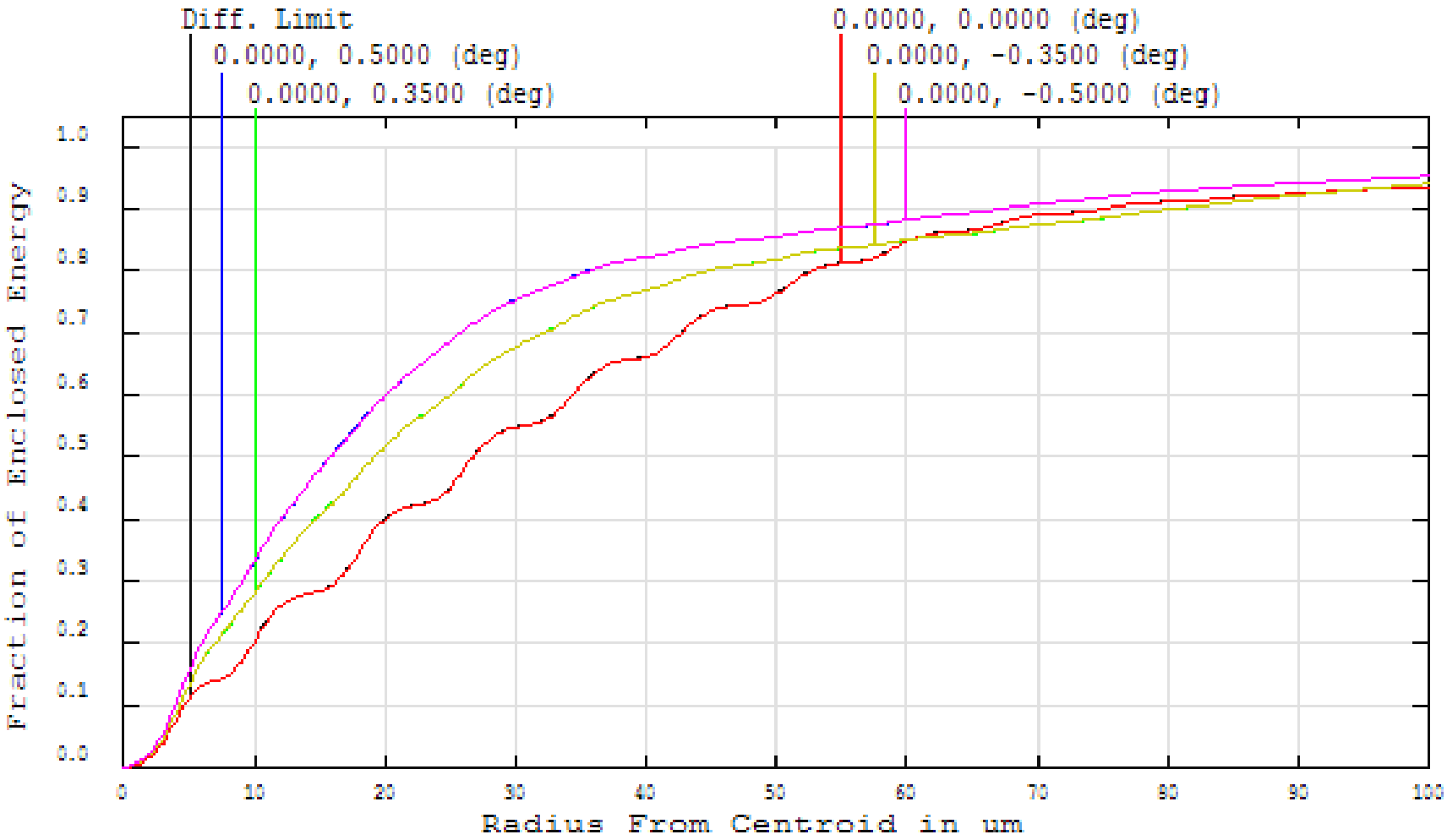

Figure 2. Variation of encircled energy with field.

the cosine of zenith angle. At zenith pointing this force equals the full weight of mirror and becomes zero at horizon. Ideally, to minimize mirror deformation, the axial supports should provide a nearly uniform pressure over the entire back surface of the primary mirror. Design criteria implemented in axial supports was to divide the mirror into sections of equal weight, each supported at its centroid. Hence the groups of three adjacent support points were supported by triangles, which in turn were supported at their centroids. Eighteen axial supports were arranged in two concentric circles to take weight acting along axis of the mirror. Thus eighteen axial supports give a geometrically sound arrangement and consist of two imaginary portions consisting of inner circle and outer circle. So the radius of equilibrium of each was determined and twelve supports were spaced in outer circle and six under inner circle. Thus one-third weight of the mirror, that is, 60 kg is taken by six supports in inner circle and

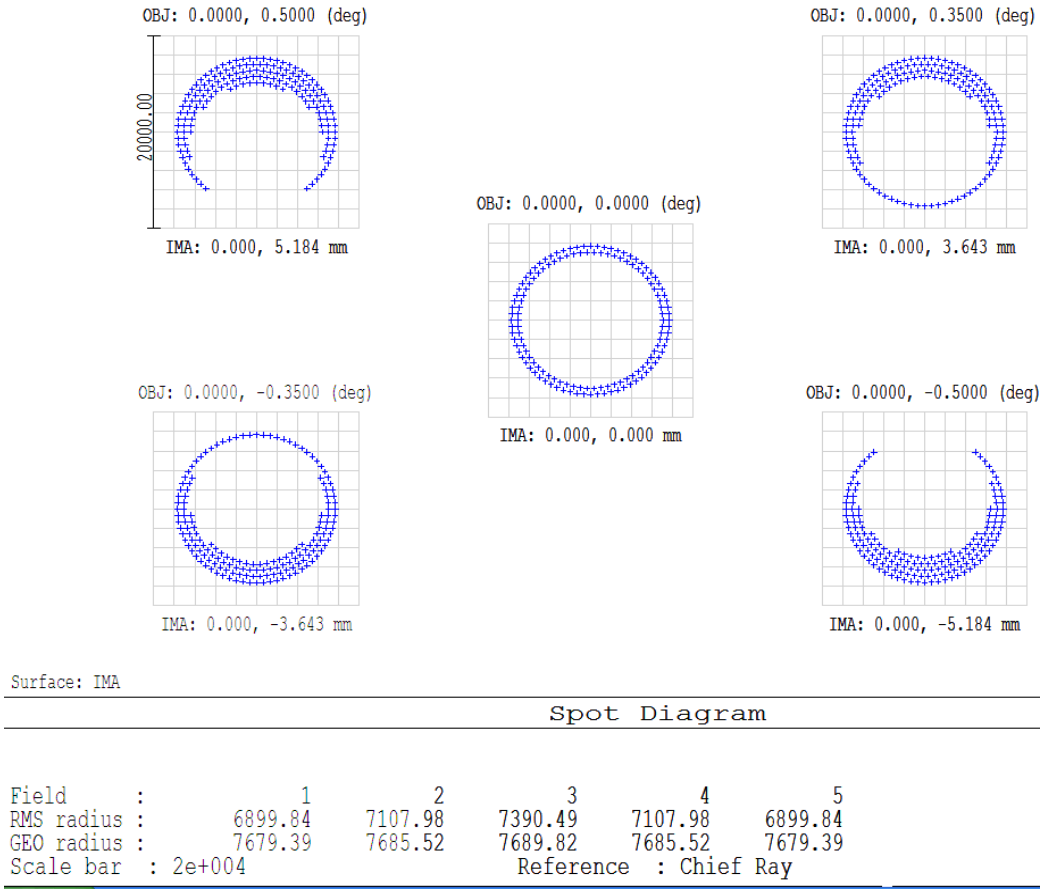

Figure 3. Spot diagrams for the variation in fields.

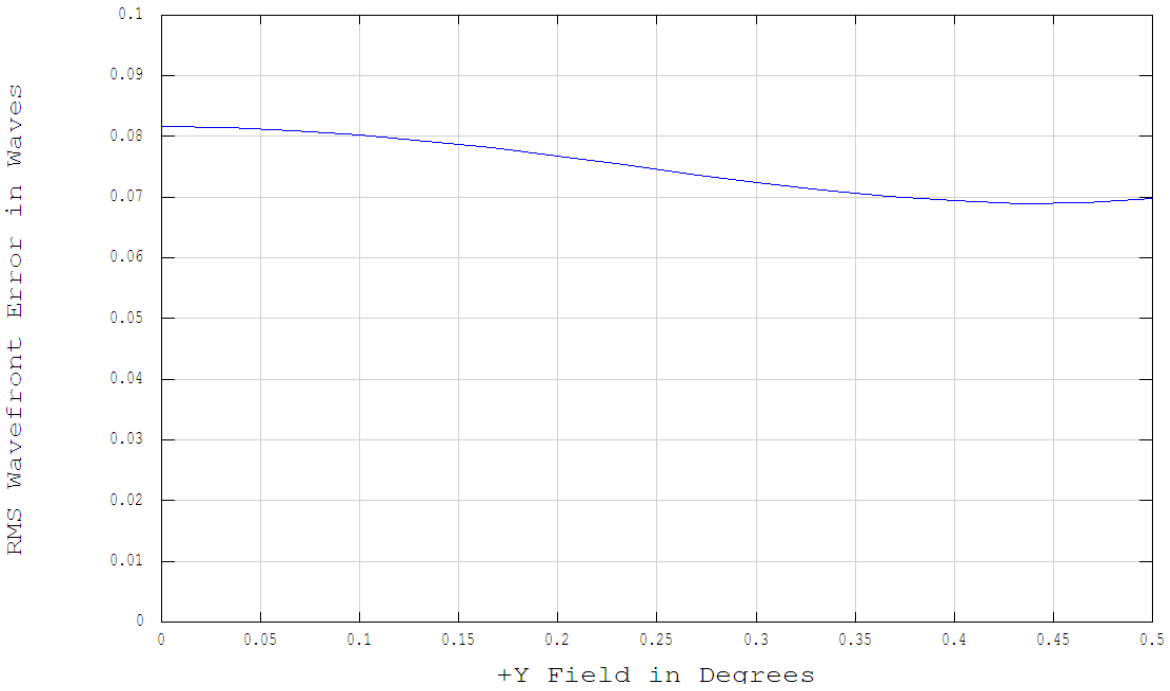

Figure 4a. Variation of RMS wavefront error in waves with field.

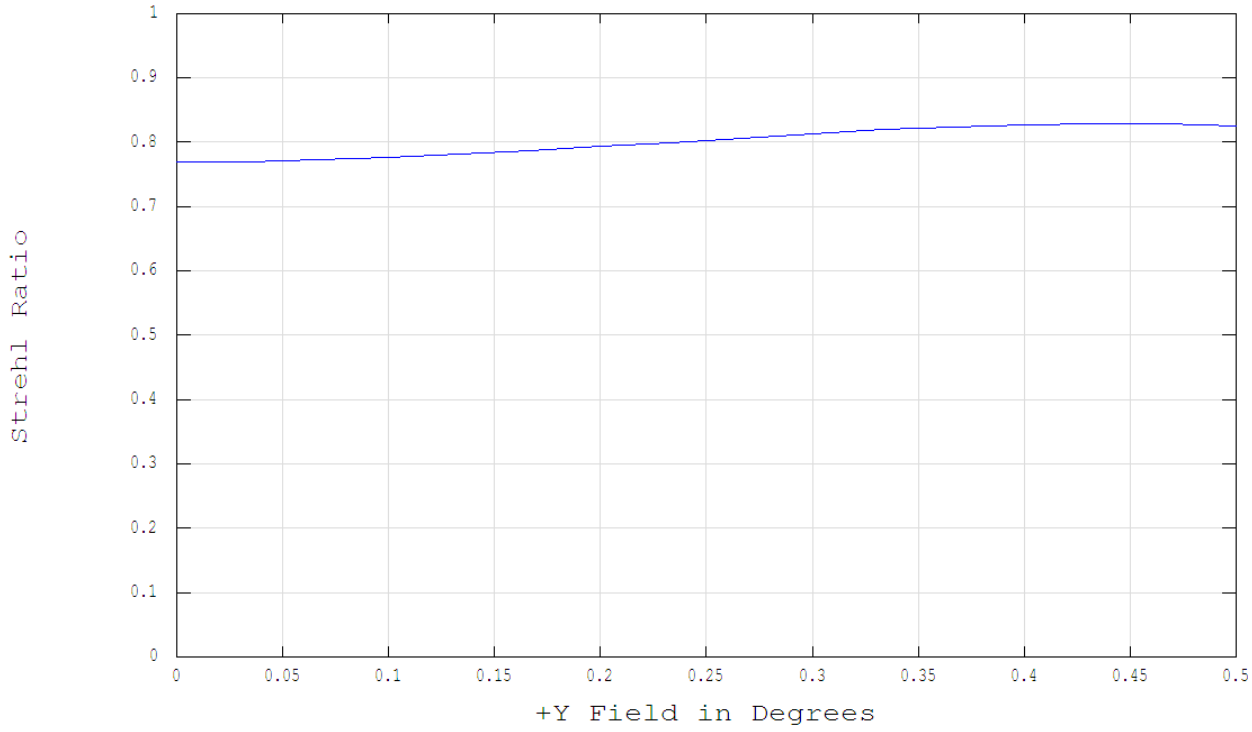

Figure 4b. Variation of Strehl ratio with field.

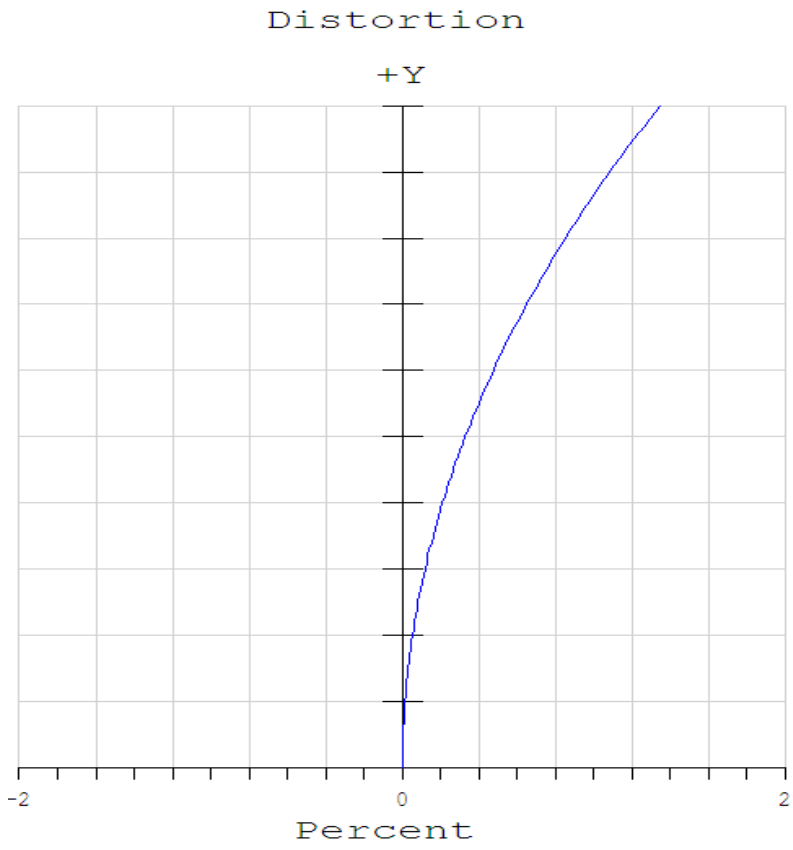

Figure 4c. Distortion curve.

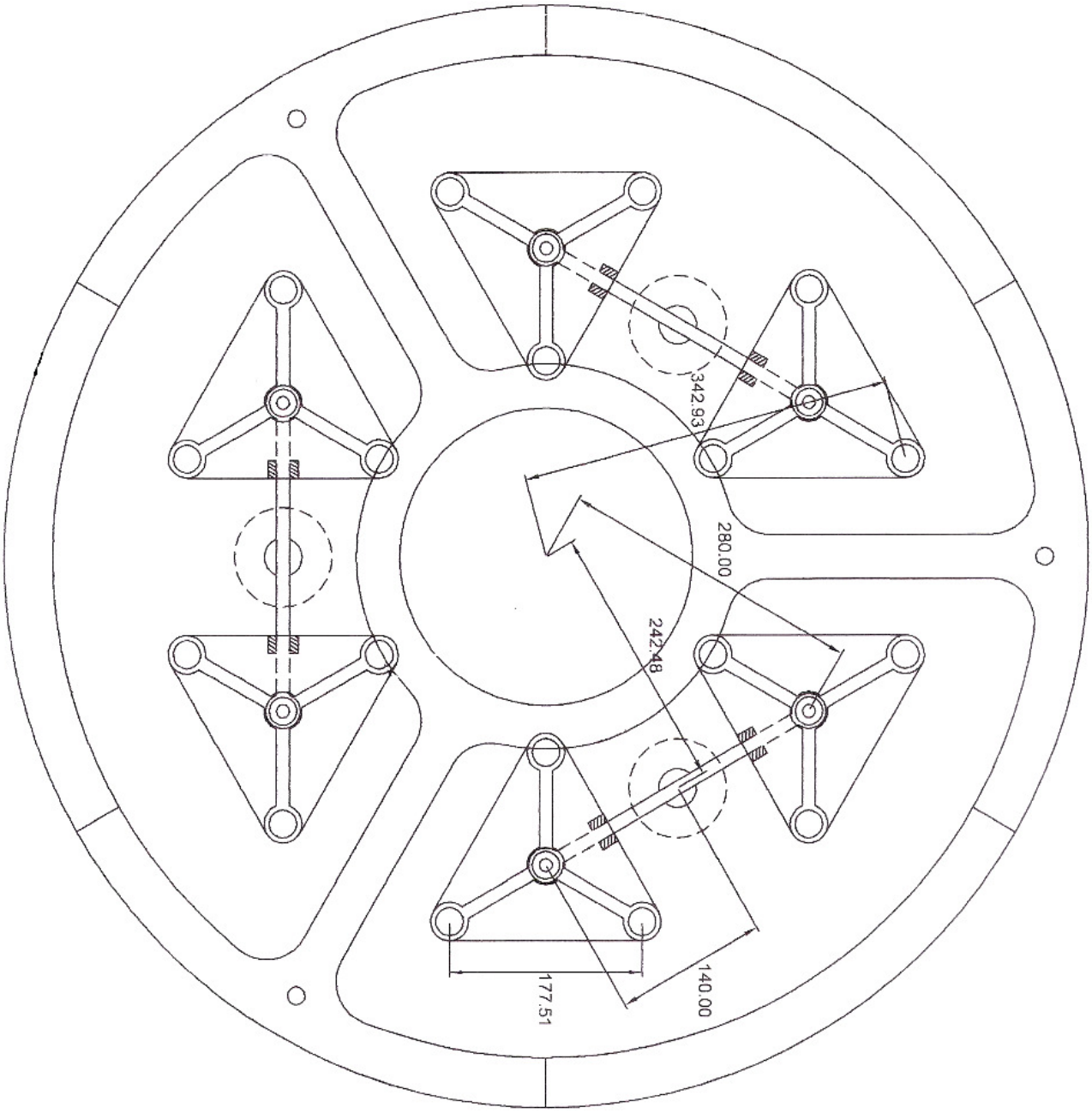

Figure 5. Axial supports arrangement for primary mirror.

two-third of the mirror weight, that is, 120 kg is taken by twelve supports in outer circle. Hence axial support system was ideally designed with each support point taking equal weight of mirror. Group of three supports, two from outer circle and one from inner circle makes a perfect equilateral triangle.

Design calculations to match positional geometry of supports were carried out for the 18 point support system (Hindle, 1996) to support 840 mm diameter (D) of primary mirror.

(i) Diameter of equilibrium of outer circle (Doc) = $\sqrt{2}D^2/3$ = 685.85 mm.
(ii) Distance between outer ring of supports (S) = Doc Sin15° = 177.51 mm.
(iii) Radius to center of 3-point triangular support (R) = D/3 = 280.00 mm.
(iv) Radius of Primary three point support (L) = R Cos30° = 242.48 mm.

The twelve supports were arranged in outer circle and six in inner circle to form six equilateral triangles (Figure 5). Six numbers of three point supports were designed and manufactured from cast aluminium alloy 535.0 by LFC process. They were held in mild steel support base brackets machined on milling machine. Steel balls of 25 mm diameter at 18 locations take and distribute weight of the mirror acting along its axis over the supports. All supports were machined to meet the design requirements.

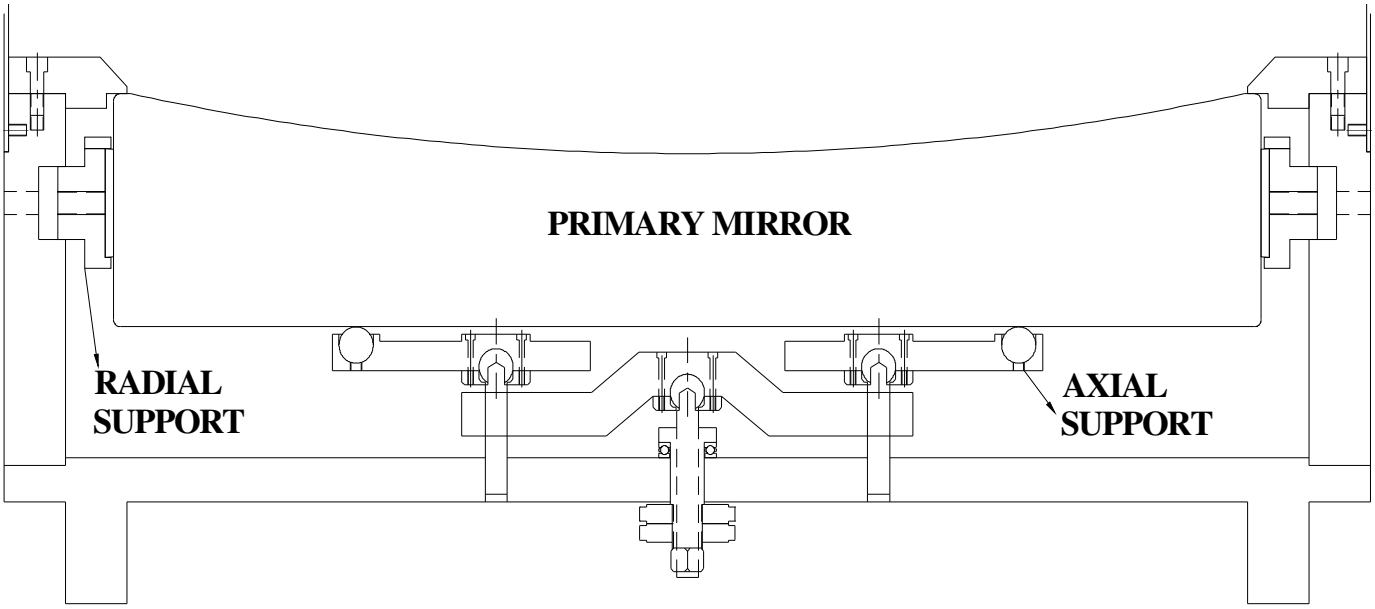

Figure 6. Primary mirror held with axial and radial supports in cell.

Radial supports for the primary mirror

Radial supports take weight acting along axis perpendicular to axis of the mirror. Total force provided by the radial supports varies as the sin of zenith angle. At zenith pointing force is zero and increases to equal the full weight of mirror at horizon. As receiver telescope will always remain vertical for LIDAR observations so radial supports will not be loaded during observations. Six radial supports of radius 420 mm from cast nylon were manufactured and assembled on circumference of the primary mirror through primary mirror cell. Cast nylon 6 of grade: Garflon 1115 of Garware synthetics Ltd. was used which has good machinability and impact strength. Patterns for radial supports were prepared taking in to consideration the shape and dimensional accuracies. Primary mirror was assembled and leveled in the primary mirror cell with 18 axial and 6 radial supports (Figure 6).

Secondary mirror mount

An elliptical mirror of 485 × 375 × 18.5 mm was used as secondary mirror in receiver telescope. A clear aperture of 475 × 335 mm was required after fitting it in its cell. A secondary mirror cell with five-axis motion using gimbals arrangement was designed to facilitate its alignment with primary mirror. It was designed with ± 5 mm motion in X and Y axis while it has ± 20 mm movement in Z axis. Angular tilt in X and Y axis were provided up to ± 5° for optical alignment.

Mount was designed with gimbal arrangement having Z movement barrel, X-Y lead screw, secondary mirror holding plate, Y movement base, X movement base and wedges were all assembled in the secondary mirror mounting spiders. Mounting spiders were held in the tube of receiver telescope to form Newtonian configuration. Elliptical mirror was mounted in its cell provided with gimbal arrangement (Figure 7). All components of secondary mirror mount were manufactured to meet the design requirements using aluminium, mild steel and SS304 grade of stainless steel. Components were dull black anodized to avoid reflection from surfaces during observations at night.

Tube and cover

The mirrors in their cells or mounts and the eye piece holder need supporting, and this is conventionally done by means of a tube (Kitchin, 1995). A tube of 1220 mm length for receiver telescope was fabricated from 3 mm thick stainless steel sheet of SS304 grade, which was TIG (tungsten inert gas) welded (Little, 1985) to form a diameter of 996 mm. Tube was fitted on the primary mirror cell through the groove provided in it to a depth of 50 mm and screwed to it all around. It was provided with two diametrically opposite windows of 300 × 200 mm at the bottom for periodic cleaning of primary mirror. Secondary mirror assembly resting strip for spiders was welded to top end of the tube. Tube was provided with a hole of 100 mm diameter opposite to the secondary mirror for mounting of detection optics system.

During day time and when night time observations are not possible due to bad weather conditions, telescope is required to be covered by a removable cover to protect optics inside it. The cover was required to be light in weight and easy to handle by a single observer at night. So a cover of 1040 mm diameter with 1.0 mm thick aluminium sheet was designed and fabricated to cover the telescope. Various sub-assemblies of LIDAR receiver telescope were assembled and connected to detection optics and electronics for taking night observations from the system (Figure 8).

RESULTS

Deflection analysis of axial supports

Axial supports design should be stiff to support the primary mirror weight and flexible enough to provide the floatation of mirror on its supports. Solid modeling of axial supports was carried out in Pro-engineer software (Figure 9a) before manufacturing. Static analysis was carried out in mechanical software of Pro-engineer for calculating deflection on supports due to weight of the mirror.

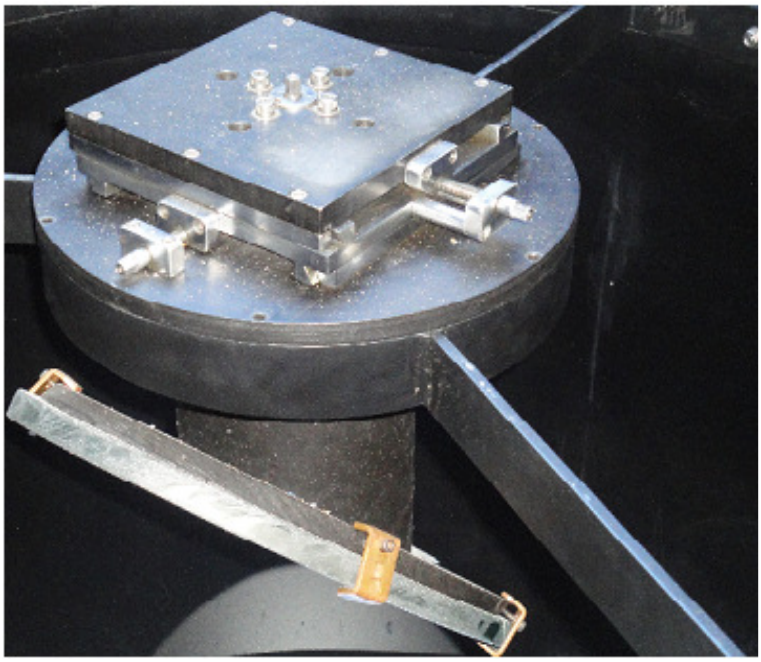

Figure 7. Secondary mirror in its cell with gimbal arrangement.

Figure 8. Assembled LIDAR receiver telescope with detection optics and electronics.

Results of analysis confirmed that maximum value of deflection on support is less than 10 µ (Figure 9b). Low deflection values will not appreciably affect the image quality of telescope and thus verified axial support system design. From the deflection analysis it was concluded that deflection on supports due to weight of mirror was mostly within 5 µ and maximum values were also below 10 µ.

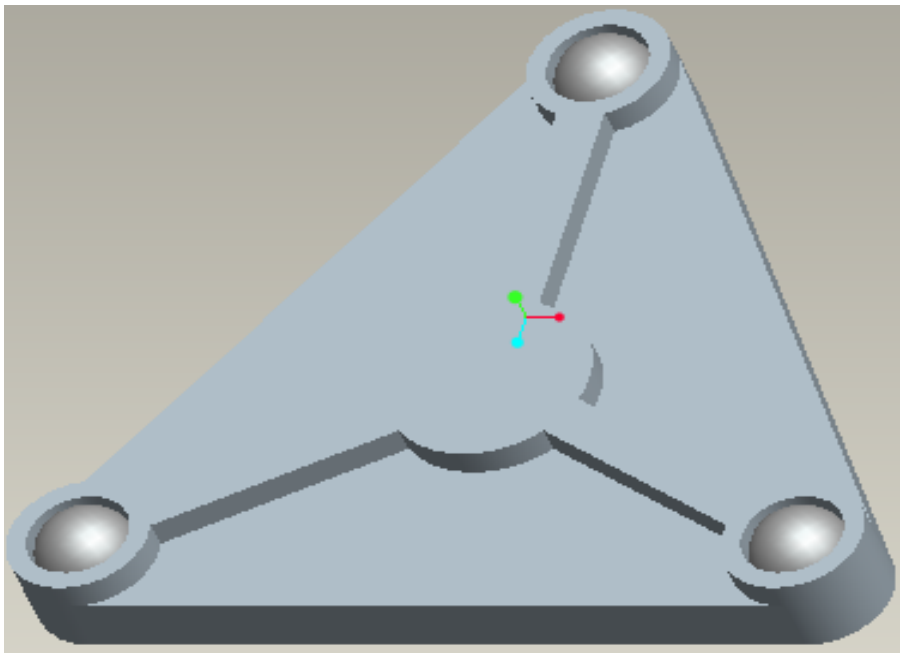

Figure 9a. Solid modeling of axial support.

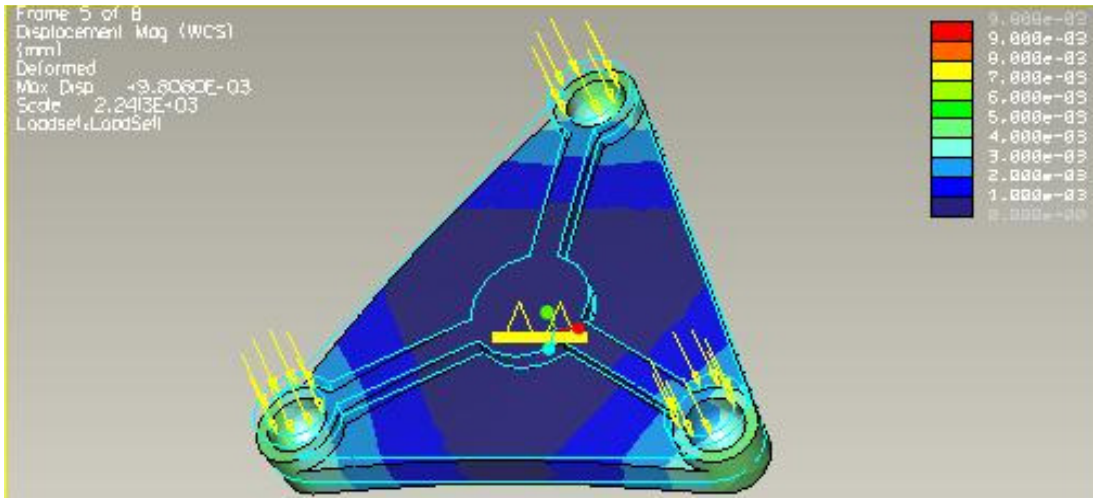

Figure 9b. Deflection analysis for axial support.

Optical analysis at deflection of 5 and 10 µ

Optical analysis at deflection of 5 and 10 µ was carried out to calculate encircled energy, spot diagrams, variation of RMS wavefront error and distortion. Variation of encircled energy was analyzed at 0.00, 0.35 and 0.50° fields. From the analysis it was found that 80% of encircled energy at 0.00° field lies in 52.99 and 59.75 µ radius for deflection of 5 and 10 µ, respectively (Figures 10a and b).

Spot diagrams for three fields at 0.00, 0.35 and 0.50° were analyzed. RMS spot size varied from 7334.21 to6842.68 µ and from 7149.27 to 6654.78 µ for deflection of 5 and 10 µ, respectively (Figures 11a and b). GEO radius varied from 7668.80 to 7659.47 µ and from 7592.16 to 7582.09 µ for deflection of 5 and 10 µ, respectively (Figures 11a and b).Variation of RMS wavefront error in waves with variation in field from 0.00 to 0.50° was computed and found to vary marginally from 0.102 to 0.090 and from 0.123 to 0.110 waves for deflection of 5 and 10 µ, respectively (Figures 12a and b).Strehl ratio changed from 0.664 to 0.730 and from 0.547 to 0.626 for deflection of 5 and 10 µ, respectively (Figures 13a and b).

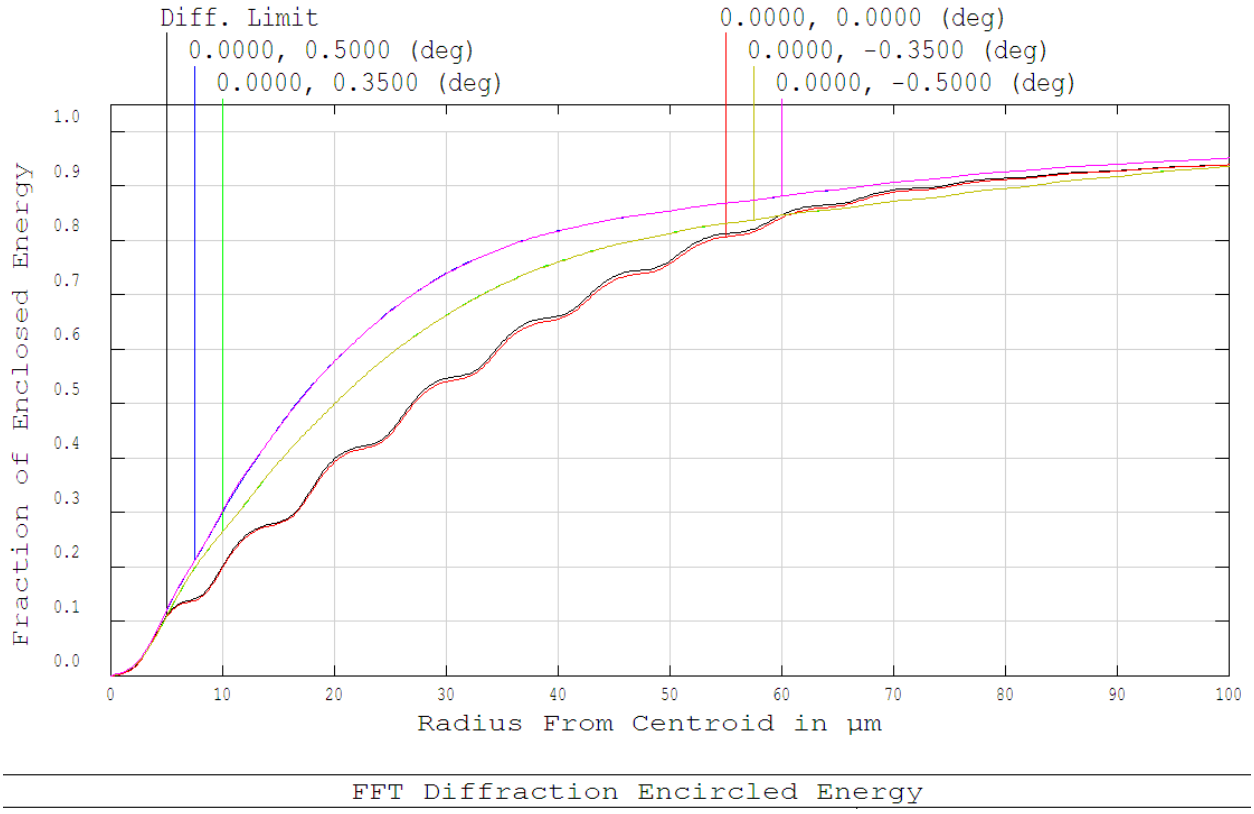

Figure 10a. Variation of encircled energy with field at 5 µ.

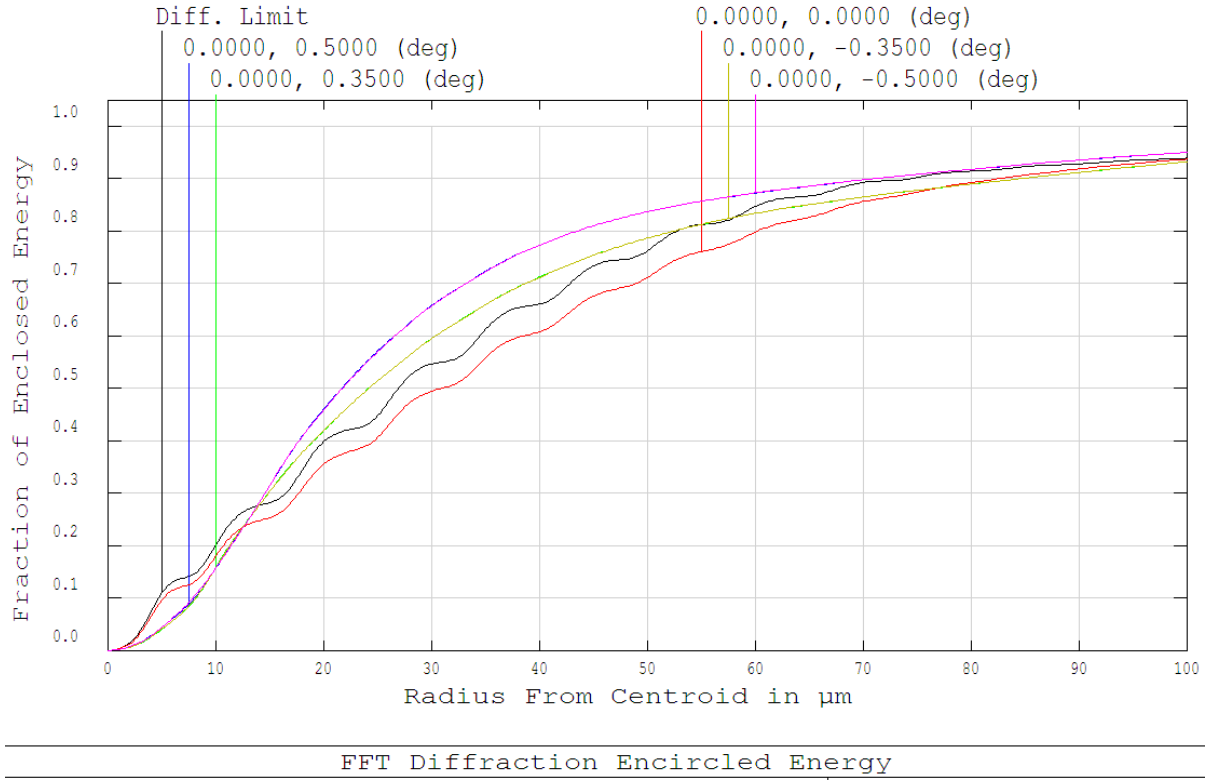

Figure 10b. Variation of encircled energy with field at 10 µ.

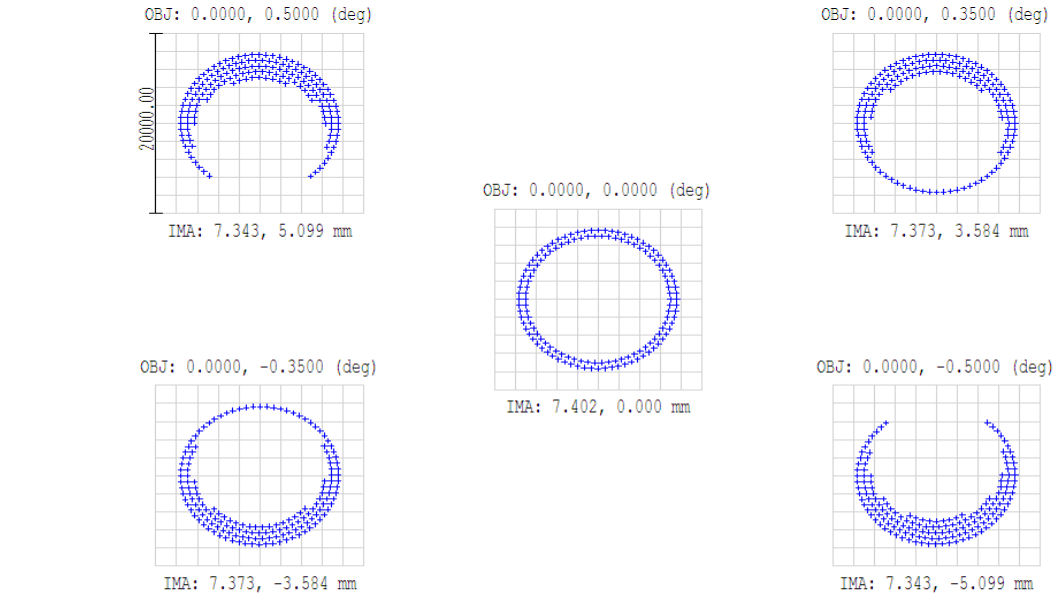

Field	:	1	2	3	4	5
RMS radius	:	6842.68	7052.47	7334.21	7052.47	6842.68
GEO radius	:	7659.47	7665.19	7668.80	7665.19	7659.47

Figure 11a. Spot diagrams for variation in fields at 5 µ deflection.

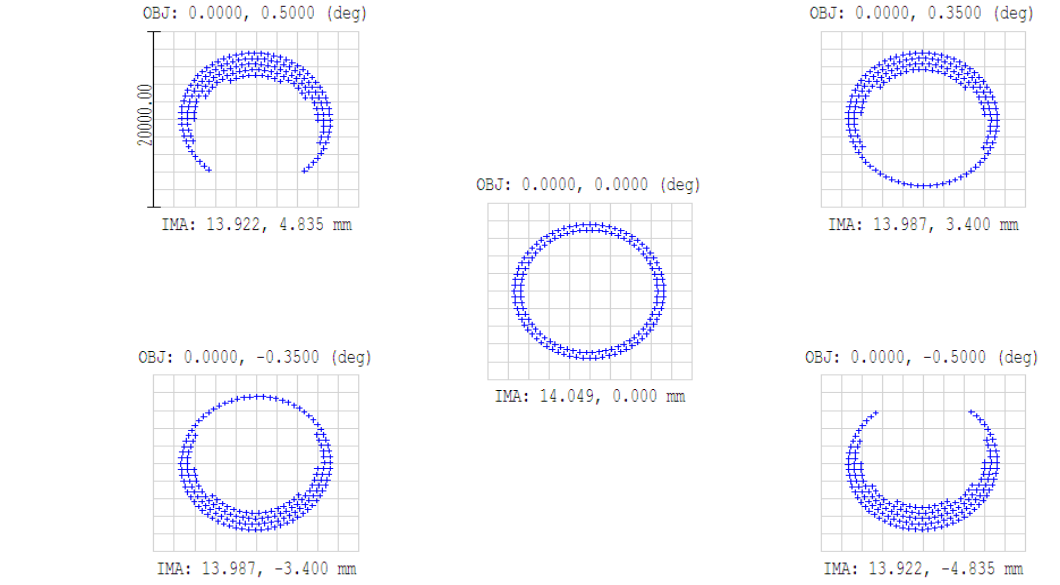

Field	:	1	2	3	4	5
RMS radius	:	6654.78	6870.06	7149.27	6870.06	6654.78
GEO radius	:	7582.09	7587.98	7592.16	7587.98	7582.09

Figure 11b. Spot diagrams for variation in fields at 10 µ deflection.

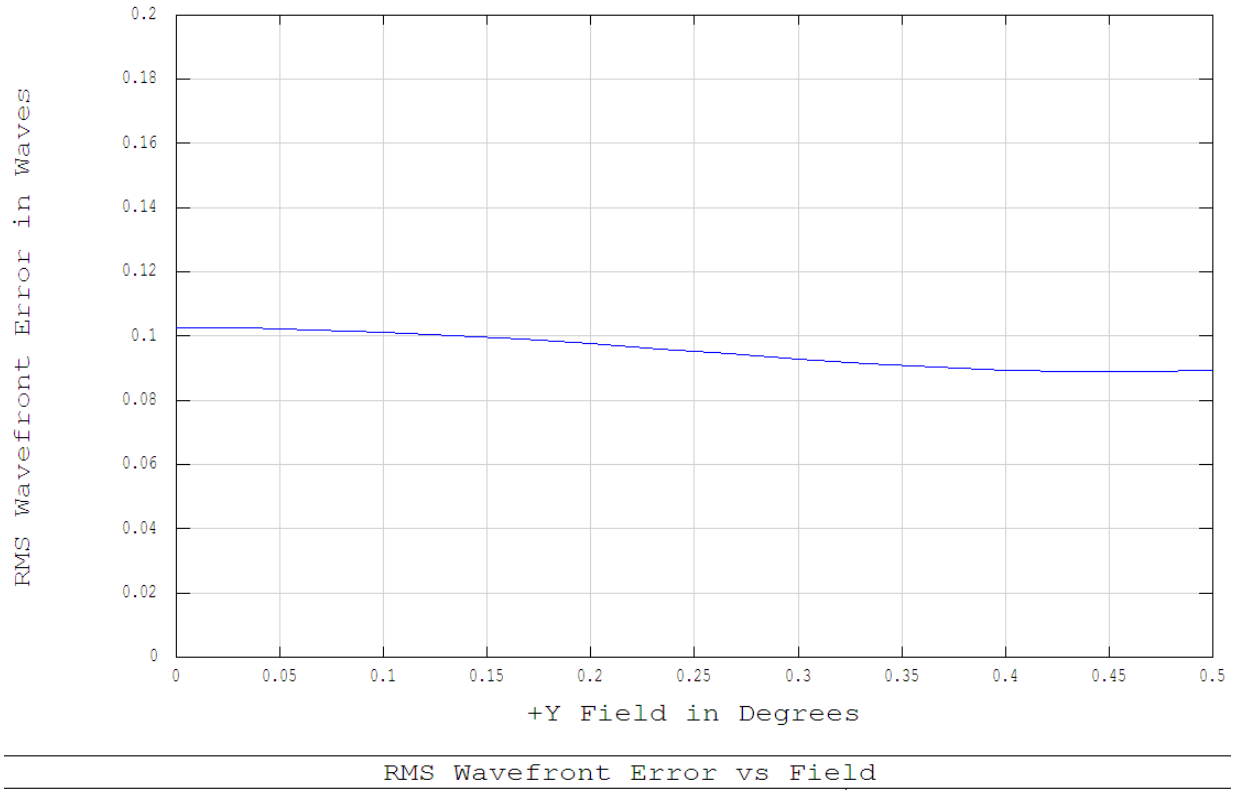

Figure 12a. Variation of RMS wavefront error in waves with field at 5 µ deflection.

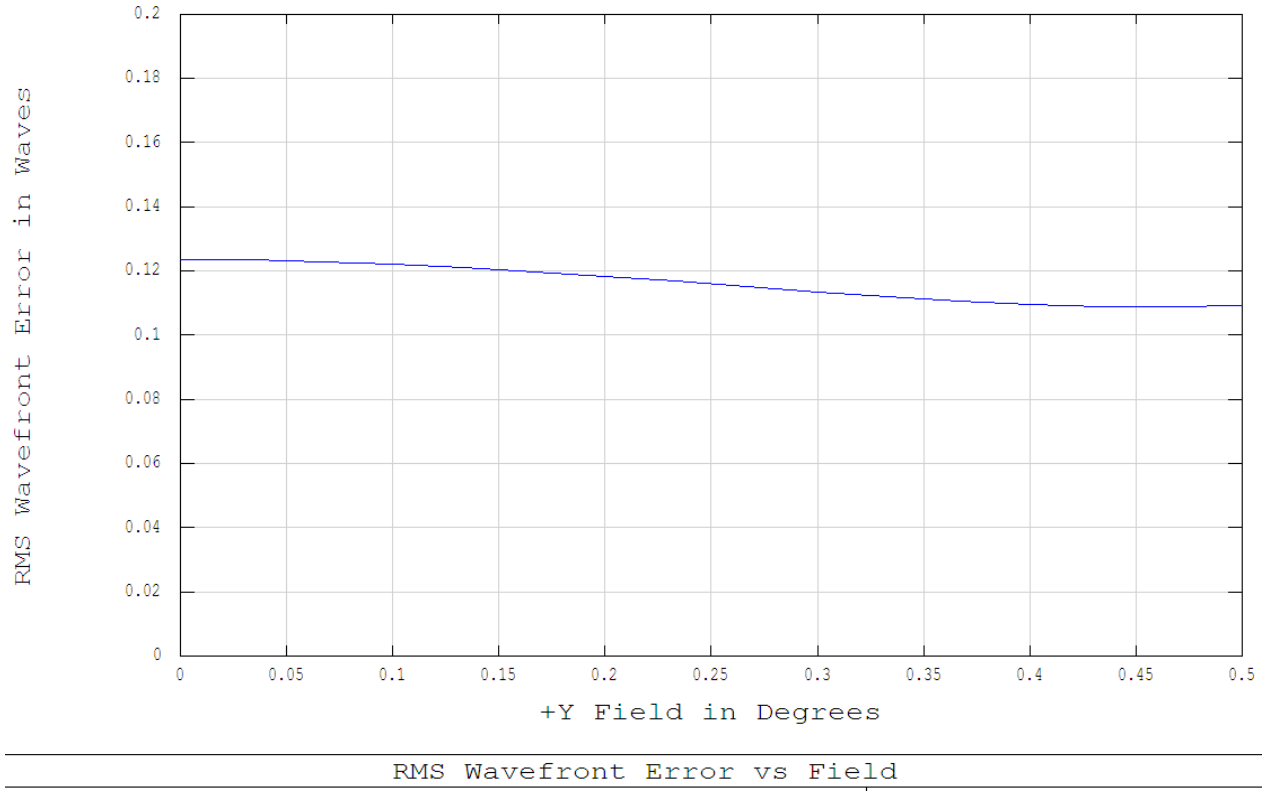

Figure 12b. Variation of RMS wavefront error in waves with field at 10 µ deflection.

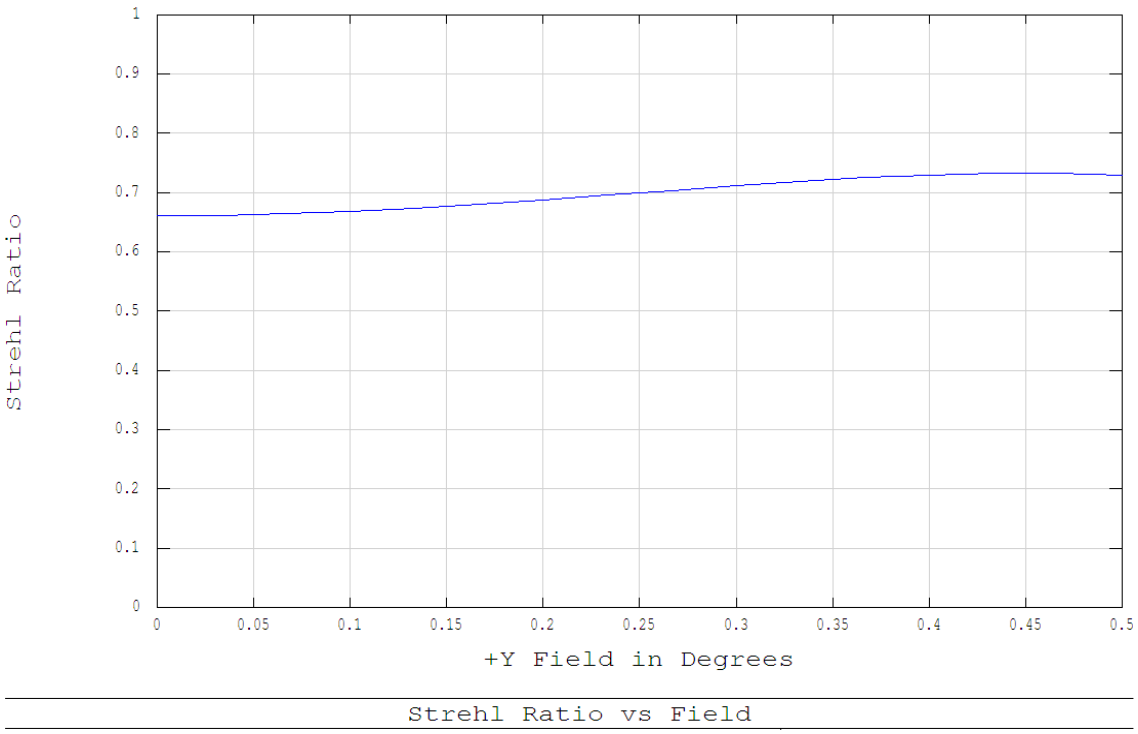

Figure 13a. Variation of Strehl ratio with field at 5 µ deflection.

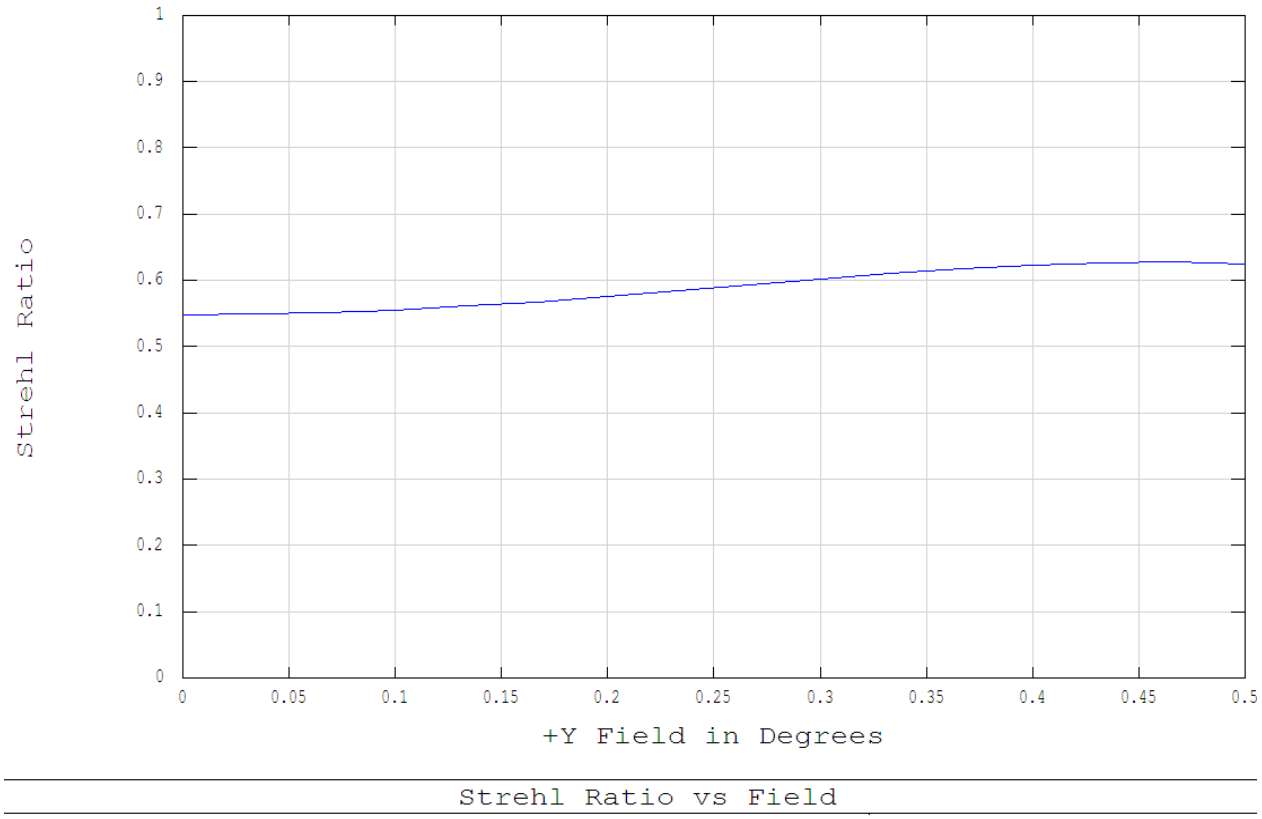

Figure 13b. Variation of Strehl ratio with field at 10 µ deflection.

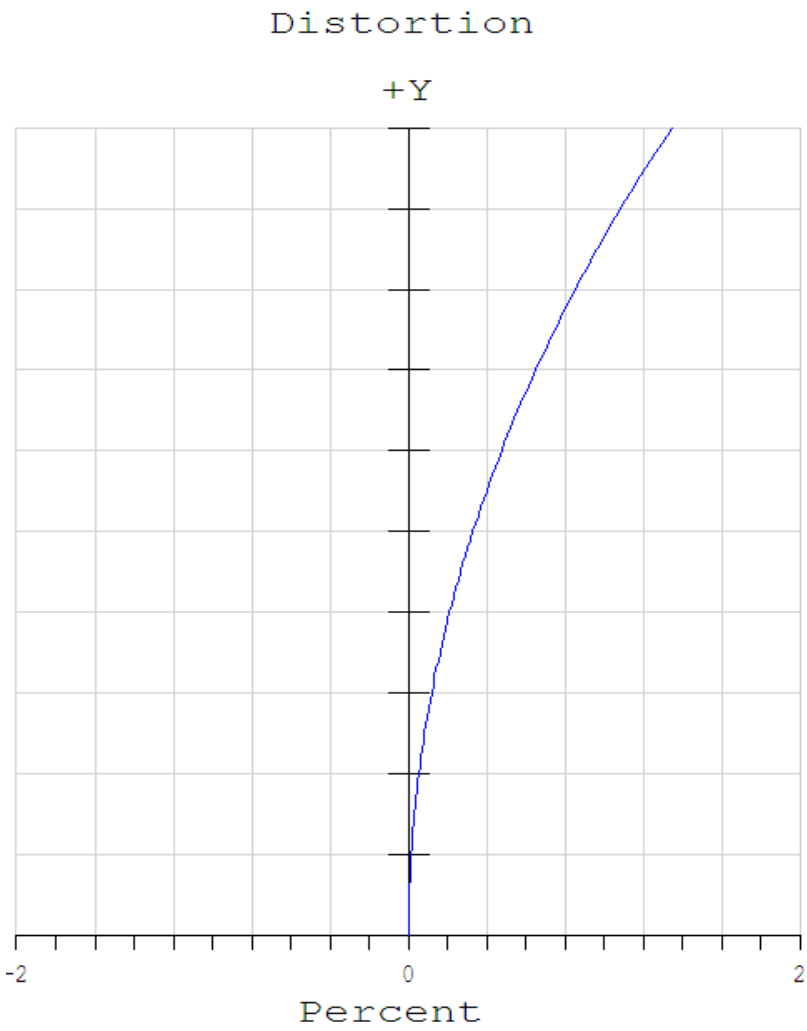

Figure 14a. Distortion curve at 5 µ deflection.

Distortion was determined as 1.32 and 1.33% for deflection of 5 and 10 µ, respectively (Figures 14a and b).

DISCUSSION

Large aperture receiver telescopes are quite beneficial for both ground (Kumar et al., 2006) and space (Simonetti et al., 2010) based LIDAR applications. They permit us to decrease the necessary LASER power which is inversely proportional to the aperture size. However large aperture receiver telescopes are quite heavy with complex designs and expensive to manufacture with monolithic mirrors. Another method of reducing cost of large aperture telescopes is the use of short focal length (Isobe, 1988). Optical simulation and optimization studies of LIDAR systems using ray tracing codes (Freudenthaler, 2003) and ZEMAX software (Kokkalis et al., 2009) have proved to be quite valuable in past. The optical design analysis of Newtonian receiver telescope and back end optics in ZEMAX-EE software, utilizing the short focal length of primary mirror proved to be quite useful in optimizing the system parameters. Encircled energy analysis shows that spread of 80% of encircled energy increases to 1.2% at 5 µ and 14.1% at 10 µ deflection at 0.00° field. A decrease of 0.76% in RMS radius at 5 µ and 3.2% at 10 µ is observed at 0.00° field. RMS wave front error in waves shows an increasing trend at deflection of 5 and 10 µ resulting in decline of Strehl ratio from 0.768 to 0.547 at 0.00° field. Value of distortion in image varies marginally from 1.31 to 1.33% at 0.50°field. Thus it is evident from the optical analysis that minor deflection in the designed axial supports will not appreciably affect the image quality of the receiver telescope.

For most of the ground based one meter class telescopes the mirror cells are made of steel (Cheng, 2009) and are quite heavy in construction requiring multiple

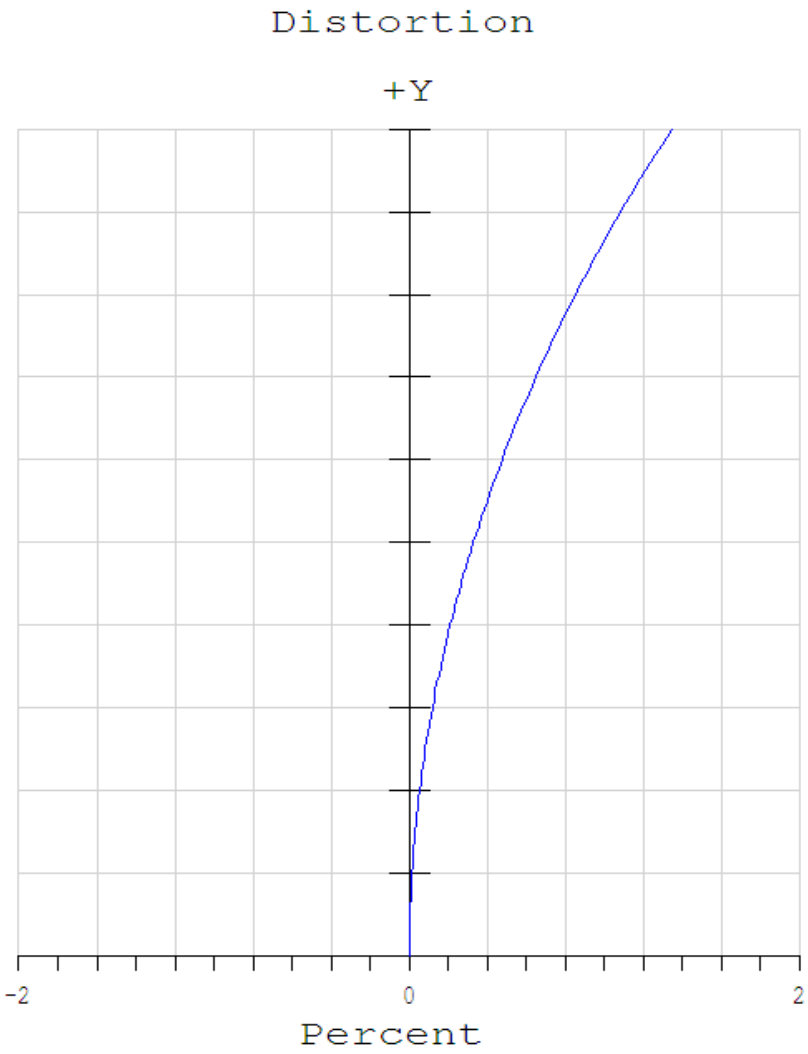

Figure 14b. Distortion Curve at 10 µ deflection.

machining operations. Light weight mechanical structure built for the fast optics of Newtonian telescope is considerably compact and cost effective. Manufacturing of mirror cell and axial supports from aluminium alloy 535.0 using LFC process resulted in tighter tolerances, weight reduction and as - cast features leading to reduction in machining and cleanup time. LFC process was invented in 1964 by M.C. Flemmings but was put to commercial use in mid 1980s for production of engine blocks, cylinder heads and crankshafts etc. by General Motors. Casting processes using aluminium alloys for manufacturing components of one meter class receiver telescope for LIDAR have not been explored much due to their inherent problems. However, LFC process provides dimensional accuracy with excellent surface finish. Also very few casting defects are observed in case of aluminium alloy castings of section thickness greater than 4 mm. This process was adopted for manufacture as there is no evidence that the gases evolved from expanded polystyrene foam degradation produce gas defects in aluminium alloy castings. Thus LFC process can be well adopted for manufacturing of telescope components using aluminium alloys to reduce weight with the advantage of precision and economy. Complexity, costs, mass and overall criticalities are subsequently reduced. Manufactured LIDAR receiver telescope will be quite useful in deriving density and temperature profiles in the middle atmosphere (Hauchecorne and Chanin, 1980). Further it has potential for mobile applications (Uchino, 1991) due to its ease of assembly and alignment accompanied by light weight and rigid structure.

Conclusions

Large aperture LIDAR receiver telescope with primary mirror of 840 mm diameter has been successfully designed, analyzed and economically manufactured.

Optomechanical design features ensured long term stability, precision, durability and low manufacturing cost. The overall dimensions and technological feasibility were matched to optimize the receiver telescope configuration to correlate the optical performance with the fulfillment of all design requirements. Static analysis of axial supports established that maximum deflection on axial supports due to primary mirror is within 10 µ, which will not significantly affect the image quality of receiver telescope. LFC process using aluminium alloy 535.0 provided value addition as it reduced finish machining and decreased the overall cost. The attractive features of the manufactured LIDAR receiver telescope include deployment of efficient methods of manufacturing with cautious selection of materials employed to reduce cost and achieve precision using simplified designs and standard engineering practices. Large aperture LIDAR receiver telescope developed is first of its kind in the central Himalayan region and can contribute significantly in atmospheric studies of this highly dynamic region. The indigenously developed LIDAR receiver at ARIES, Manora Peak is ready to study atmospheric parameters from this Central Himalayan site for a better understanding of atmospheric dynamics.

ACKNOWLEDGEMENTS

We thank P Pant, A Omar, DV Phanikumar and KG Gupta for providing their valuable support. TB acknowledges the encouragement and support from the RDC committee of UPTU, Lucknow. This project is funded by Department of Science and Technology, Government of India.

REFERENCES

Bely PY (2003). The Design and Construction of Large Optical Telescopes. Springer-Verlag., New York, 220: 233.

Bhavani Kumar Y, Raju CN, Krishnaiah, M (2006). Indo-Japanese lidar observations of the tropical middle atmosphere during 1998 and 1999. Adv. Atm. Sci., 23(5): 711-725.

Boyarchuk AA, Steshenko NV, Terebizh VY (2008). Optical Layout of the T-170M Space Telescope. Bull. Crimean Ast. Obs., 104: 171-178.

Chandler H (2006). Heat treater's guide: practice and procedures for non- ferrous alloys, ASM Int., USA, p. 266.

Chanin ML, Hauchecorne A (1981). LIDAR observation of gravity and tidal waves in the stratosphere and mesosphere. J. Geophys. Res., 86: 9715-9721.

Cheng J (2009). The Principles of Astronomical Telescope Design. Springer., USA, p. 41.

Dabas RS, Sharma K, Das RM, Sethi NK, Pillai KGM, Mishra AK (2008). Ionospheric modeling for short- and long-term predictions of F region parameters over Indian zone. J. Geophys. Res., 113: A03306.

Fiocco G, Grams G (1964). Observations of the aerosol layer at 20 km by optical radar. J. Atmos. Sci., 21: 323-324.

Fiocco G, Smullin LD (1963). Detection of Scattering Layers in the Upper Atmosphere (60–140 km) by Optical Radar. Nature, 199:1275 - 1276.

Freudenthaler V (2003). Optimized background suppression in near field lidar telescopes. 6th Int. Sym. Tropospheric Profiling, Needs - and Technologies.

Hauchecorne A, Chanin ML (1980). Density and temperature profiles obtained by LIDAR between 35 and 70 Km. Geophys. Res. Lett., 7(8): 565-568.

Hindle JH (1996). Amateur Telescope making (2). Ingalls AG, ed. Willmann-Bell, Inc., USA, pp. 319-327.

Isobe S (1988). How to build cheaper telescopes? Vis. Astr., 31: 745-754.

Jayaraman A, Joshi PC, Ramesh R (2007).Developments and achievements in atmospheric sciences and space meteorology in India. Curr. Sci., 93(12): 1779-1790.

Kitchin CR (1995). Telescopes and Techniques. Springer-Verlag., London, pp. 49-55.

Kokkalis P, Georgoussis G, Papayannis A, Hatzidimitriou D, Porteneuve J, Mamouri RE, Tsaknakis G (2009). Optimization-through optical design-of a multi-wavelength fiber- based Raman-lidar system in the near field for vertical aerosol measurements in the troposphere. Proc. 8th Inter. Symp. Tropospheric Profiling, S06: 1-4.

Ligda MGH (1963). Proc. First conf. laser Tech. U.S. Navy., ONR, pp. 63-72.

Little RL (1985). Welding and Welding Technology. Tata McGraw-Hill., India, 217: 227.

Liu B, Zhong, Z, Zhou J (2007). Development of a Mie scattering lidar system for measuring whole tropospheric aerosols. J. Opt. A: Pure Appl. Opt., 9: 828-832.

Meinel AB (1977). Telescopes. Kuiper GP and Middlehurst BM ed. The University of Chicago Press., USA, 1: 25-42.

Nelson JE, Lubliner J, Mast TS (1982). Telescope mirror supports: plate deflections on point supports. SPIE: Adv. Technol. Opt. Telesc., 332: 212-228

Niemann EH (1998). Expandable Polystyrene Pattern Material for the Lost Foam Process. AFS Trans., 96: 793-798.

Pillai KGM, Dabas RS, Veenadhari B, Lakshmi DR (2003). The scientific basis for Solar-terrestrial predictions at National Physical laboratory, New Delhi. J. Ind. Geophys. Union, 7(3): 159-165.

Sagar R (2006). Aryabhatta Research Institute of Observational Sciences: reincarnation of a 50 year old State Observatory of Nainital. Bull. Astro. Soc. India, 34: 37-64.

Sagar R, Kumar B, Dumka UC, Moorthy KK, Pant P (2004) Characteristics of aerosol spectral optical depths over Manora Peak: A high-altitude station in the central Himalayas. J. Geophys. Res., 109: D06207.

Schwab IR (2003). Mirrors at the birth of Aphrodite. Br. J. Ophthalmol., 87: 1311.

Simonetti F, Marchi AZ, Gambicorti L, Bratina V, Mazzinghi P (2010). Large aperture telescope for advanced laser systems. Opt. Eng., 49(7): 073001.

Uchino O, Tabata I (1991). Mobile lidar for simultaneous measurements of ozone, aerosols, and temperature in the stratosphere. App. Opt., 30(15): 2005-2012.

Velotta R, Bartoli B, Capobianco R, Fiorani L, Spinelli N (1998). Analysis of the receiver response in lidar measurements. App. Opt., 37(30): 6999-7007.

Waghmare SY, Carlo L, Gawali PB, Patil AG (2008). Geomagnetic investigation in the Seismoactive area of Narmada-Son Lineament, Central India. J. Ind. Geophys. Union, 12(1): 1-10.

Weitkamp C (2005). Lidar: Range Resolved Optical Remote Sensing of the Atmosphere. Springer., New York, pp. 1-4.